ACADEMIC PRESS

Available online at www.sciencedirect.com
SCIENCE DIRECT®

Journal of Catalysis 216 (2003) 313–323

JOURNAL OF CATALYSIS

www.elsevier.com/locate/jcat

Common mechanistic aspects of liquid and solid acid catalyzed alkylation of isobutane with *n*-butene

Andreas Feller, Iker Zuazo, Alexander Guzman, Jan O. Barth, and Johannes A. Lercher *

Institut für Technische Chemie, Technische Universität München, Lichtenbergstrasse 4, D-85748 Garching, Germany

Received 29 July 2002; revised 18 September 2002; accepted 19 September 2002

Abstract

Recently developed mechanistic and technological concepts concerning the isobutane/butene alkylation reaction on liquid and solid acids are addressed. Differences and similarities between the reactions of alkenes and alkanes with these acids are emphasized. Hydride transfer is shown to be the important step for high catalyst productivity and product quality. High concentrations of strong Brønsted acid sites and low concentrations of Lewis acid sites are mandatory for long catalyst life. Deactivation in liquid and solid acids proceeds through the formation of highly unsaturated compounds, which form strong complexes with the acid sites. Implications of the most important process parameters on the alkylation performance are discussed.

1. Introduction

Alkylation of isobutane with C_3–C_5 alkenes is of considerable economic importance for the production of high-octane gasoline with low residual vapor pressure that is virtually free of aromatic and sulfur-containing compounds. The reaction is catalyzed by strong acids, of which only sulfuric and hydrofluoric acid are commercially used. The worldwide alkylation production capacity at the end of 2001 amounted to 1.8 million barrels per calendar day (∼ 74 million tons/year). Slightly more than half of the total is produced with hydrofluoric acid as catalyst [1].

Both acids suffer from certain drawbacks. Anhydrous hydrofluoric acid is a corrosive and highly toxic liquid with a boiling point close to room temperature. Released into the atmosphere, it forms aerosols, which drift downwind at ground level for several kilometers. For that reason, alkylation plants working with HF have to be equipped with expensive safety measurements to prevent leakage of HF to the outside. Sulfuric acid also is a corrosive liquid, but not volatile, which makes its handling easier. Its major disadvantage is the high acid deactivation, which may amount to 70–100 kg acid/ton alkylate. About one-third of the total operating costs of alkylation units using H_2SO_4 is attributed to acid consumption [2].

Zeolites were the first solid acids tested as alternatives to sulfuric and hydrofluoric acid in isobutane/alkene alkylation. The pioneering work was reported by researchers at Sun Oil [3] and Mobil [4] in late 1960. In addition to zeolites, Brønsted and Lewis acids on various supports, heteropolyacids and organic resins, both supported and unsupported, have been examined as catalysts for alkylation. Rapid catalyst deactivation through a buildup of oligomers blocking the sites/pores is common to all solid acids. Therefore, an economically competitive process has to include a regeneration section. So far, no process utilizing a solid acid is operative on an industrial scale, although some companies offer their developed processes for licensing [5,6].

The technology and chemistry of isoalkane–alkene alkylation have been thoroughly reviewed in the past for both liquid and solid acid catalysts [7] and for solid acid catalysts alone [8]. Since that time, our knowledge about acid-catalyzed hydrocarbon reactions both in liquid and on solid acids has advanced. With the existing alkylation processes being mature technologies, the number of publications on sulfuric and hydrofluoric acid is considerably smaller than that on solid acids. Nevertheless, trifluoromethanesulfonic acid (triflic acid) as an alternative strong liquid acid has received particular attention in mechanistic studies. Here, we describe the elements which we believe

* Corresponding author.
E-mail address: johannes.lercher@ch.tum.de (J.A. Lercher).

0021-9517/03/$ – see front matter
doi:10.1016/S0021-9517(02)00068-4

to be important in understanding the mechanism of liquid- and solid-acid-catalyzed alkylation, including our own recent work [9,10].

2. On the interaction of alkanes and alkenes with strong acids

Chemical bonding of alkenes with strong liquid Brønsted acids is usually described as occurring via π-bonding of the olefins to the acid hydroxyl group followed by protonation to yield a free alkyl carbenium ion. The role of the negative counterion (sulfate or fluoride ion) is largely neglected. While this is permissible for emphasizing the main catalytic features, it does not reflect the reality in the ground state. The reaction of *n*-alkenes with sulfuric or hydrofluoric acid leads to mono and dialkyl sulfates or alkyl fluorides. Similarly, triflic acid (CF_3SO_2OH) forms alkyl triflates [11]. These esters are stable at low temperatures and low acid/hydrocarbon ratios. With a large excess of acid, the ester will decompose and form corresponding carbenium ions:

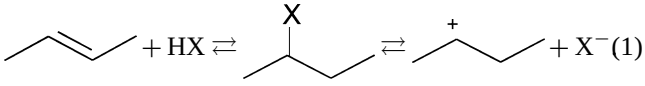

(1)

The esters differ in stability. To decompose the isopropyl ester, higher temperatures and higher acid strengths are needed than for the decomposition of the *sec*-butyl ester. It is claimed that the resulting carbenium ions are stabilized by solvation through the acid [12–14]. Branched alkenes do not form stable esters. It is thus concluded that isoalkenes easily protonate and polymerize [15].

Correspondingly, the adsorption of alkenes onto zeolites leads to the formation of a surface alkoxy group and not to a free carbenium ion. The alkyl fragment may be further stabilized by surrounding basic surface oxygen atoms in the vicinity of the acid site. Depending on the base strength of these oxygens, more or less covalent surface alkoxides are formed [16,17]. Ab initio quantum chemical calculations on a cluster representing the zeolitic acid site [16,18] showed that the alkene first forms a π-complex with the acid site. This transforms into the alkoxide via a carbenium ion transition state. The transition state has a much higher positive charge than the alkoxide and it forms a cycle with both oxygen atoms and the aluminum atom. Interestingly, the alkoxy group formed will not bind to the oxygen to which the proton of the Brønsted acid site was connected. The involvement of more than one oxygen atom and the mobility of the carbenium ion between them are characteristic of hydrocarbon transformations on zeolite acid sites [19]. For the sake of clarity and because all transformations pass through the carbenium ion in the activated state, all reaction intermediates will be called carbenium ions in the following, irrelevant of their true nature.

Let us now turn to the activation of the alkane. The direct protonation of isobutane, via a pentacoordinated carbonium ion, is not likely under typical alkylation conditions. This reaction would lead to a tertiary butyl carbenium ion and hydrogen, or a secondary propyl carbenium ion and methane [20–22]. With zeolites, this reaction starts to be significant only at temperatures above 200 °C. At lower temperatures, hydrocarbon transformations start with the activation of the most reactive alkene [23], while alkanes enter the reaction cycles through hydride transfer.

Theoretically, the direct alkylation of isobutane by carbenium ions is also feasible. The reaction of isobutane with a *tert*-butyl would lead to 2,2,3,3-tetramethylbutane as the primary product. With liquid superacids under controlled conditions, this has been reported [24–26], but under typical alkylation conditions 2,2,3,3-TMB is not produced.

Kazansky et al. showed evidence for the direct alkylation of isopentane with propene using a two-step alkylation experiment. In this reaction sequence, the alkene first forms an ester, which in the second step reacts with the isoalkane. Isopentane was found to directly add to the isopropyl ester via a non-classical carbonium ion as intermediate. In this way, a carbonium ion is formed from the carbenium ion and the alkane, which readily decomposes into an alkane and the free Brønsted acid site [13,14]. The absence of hydride transfer was concluded from the near absence of propane in the product mixture. Note that in these experiments great care was taken to exclude the presence of alkenes in the reaction mixture, as they would be preferentially added to the carbenium ions. In continuous operation, however, with a constant feed stream of alkenes entering the reactor, this type of reaction most likely occurs only infrequently.

3. The importance of the hydride transfer step

Intermolecular hydride transfer (2), typically from isobutane to an alkylcarbenium ion, transforms the carbenium ions into the corresponding alkanes and leads to the *tert*-butyl cation, which continues the chain sequence in liquid acids and zeolites. Hydride transfer is the crucial step in this reaction sequence, allowing the chain propagation of acid-catalyzed transformations of hydrocarbons and the formation of the saturated compounds [27]:

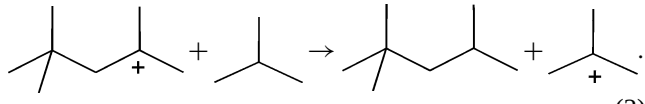

(2)

Fig. 1 displays the basic alkylation mechanism as adapted from Schmerling [28,29]. The product distribution is governed by the relative rates of three individual steps, i.e., alkene addition, isomerization, and hydride transfer. The antagonistic pair of reactions, i.e., alkene addition and hydride transfer, determine whether or not the catalyst tends to single or multiple alkylation. With all acids, alkene addition is

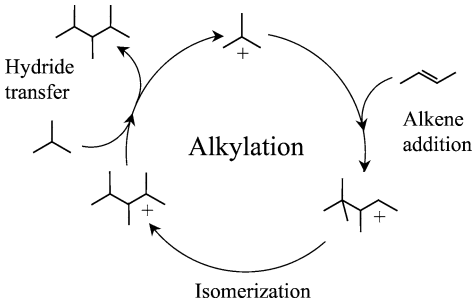

Fig. 1. Simplified alkylation cycle including the three key reaction steps of alkene addition, isomerization, and hydride transfer.

much more facile than hydride transfer. With sulfuric acid, *n*-butene oligomerization is four times faster than hydride transfer [30]. For zeolites, de Jong et al. reported oligomerization to be two orders of magnitude faster than hydride transfer [31], while Simpson et al. reported even three orders of magnitude [32]. When the true paraffin-to-olefin ratio is low, alkenes will oligomerize before they can be removed via hydride transfer. When solid acids are used, a polymer will build up via this route, which finally blocks all acid sites. For industrial realization high paraffin to olefin ratios can, for example, be achieved by employing a continuously operated well-stirred tank reactor at high conversion.

Isomerization and hydride transfer determine to what extent primary and equilibrium products are observed. Fast hydride transfer reduces the lifetime of isooctyl carbenium ions. The molecules have less time to isomerize and, consequently, the observed product spectrum should be closer to the primary products and further away from equilibrium composition. This was indeed observed when adamantane, an efficient hydride donor, was admixed to a H-BEA catalyst [33]. Using 2-butene/isobutane feed, the increased hydride transfer activity led to considerably higher 2,2,3-TMP and lower 2,2,4-TMP selectivities, as shown in Fig. 2.

While hydride transfer in the gas phase proceeds via a carbonium-ion-like transition state without activation energy [34–37], a small barrier of 13–17 kJ/mol has to be overcome in the liquid phase [12]. The difference is explained by solvation effects in the liquid phase. The carbenium ions are more efficiently stabilized by solvation than carbonium ions, because of the unsaturated trivalent carbon atom in carbenium ions. In this way, the energy barrier between the two states increases.

In zeolites, the activation barrier for hydride transfer is higher than in the liquid phase. As outlined above, the lower acid strength and the interaction between the zeolitic oxygen atoms and the hydrocarbon fragments lead to the formation of alkoxides rather than carbenium ions. Thus, extra energy is needed to transform these esters into carbenium and carbonium-ion-like active complexes. The hydride transfer step on zeolitic acid sites has been simulated by several groups using quantum chemical methods. Kazansky suggests the activation energy for isobutane/*tert*-butoxide hydride transfer to be approximately 200 kJ/mol [16]. Rigby

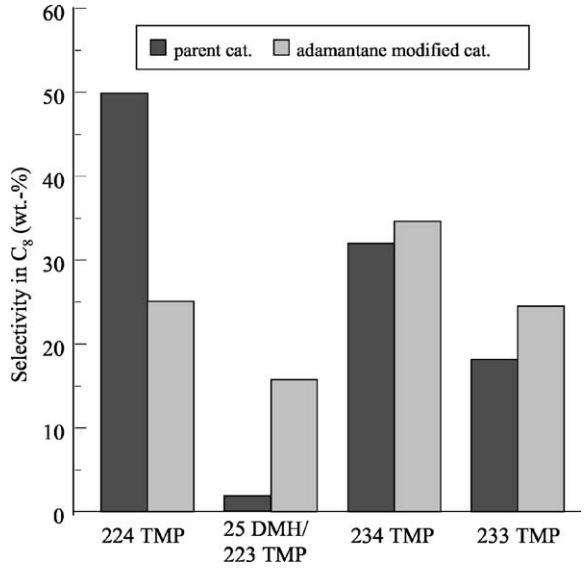

Fig. 2. Changes in TMP selectivities with the use of adamantane (5 wt%) as additive in a H-BEA catalyst at 30 min TOS. Taken from Ref. [33].

et al. [19] calculated for the same step an activation energy of 240 kJ/mol. Values of about 100 kJ/mol have been calculated for isobutane/isobutene hydride transfer by Corma and co-workers [38]. It is interesting to note that the carbonium ions in the transition state are proposed to be energetically high-lying reaction intermediates, which are stabilized when the charge is delocalized and not accessible to framework oxygen. Note that the theoretical calculations of Corma and co-workers suggest that the carbonium ions decompose directly into alkene and alkane, without the alkene forming an alkoxide. From a conceptual point of view it seems plausible that the calculated activation energies reported by Corma and co-workers [38] are $\sim$ 100 kJ/mol lower than those in the other mentioned references, because covalent bonds need not be broken to reach the transition state.

We would like to emphasize in this respect that kinetic evaluation of alkane cracking led to lower values of the energies of activation for hydride transfer than quantum chemical calculations. For i-C_4/C_n^+ hydride transfer, energies of activation in the ranges 70–125 kJ/mol [39], 62–76 kJ/mol [23], and 47 kJ/mol [40] have been reported. It should be noted, however, that these energies are apparent energies of activation and need to be corrected for the heat of adsorption of the hydrocarbons, which mainly depends on the chain length of the molecules [41] and, in case of zeolites, the framework density [42,43].

4. Requirements on strength and concentration of acids

The requirements with respect to the acid strengths and the concentrations of acid sites are complex. Sulfuric acid is a somewhat stronger acid than hydrofluoric acid; i.e., it has an H_0 value of -14.1, compared to -12.1 for the water-free acids. Note that these subtle differences may not be of marked importance, as the maximum alkylate quality

employing sulfuric acid is not achieved with the highest acidity, but with acid containing 1–1.5% water and 4–5% acid-soluble oils [44]. When the concentration of diluents exceeds a certain level, however, the acid strength is too low to produce a high quality alkylate. Sulfuric acid of 60–80% concentration catalyzes only alkene oligomerization, with its acid strength being too low to catalyze hydride transfer and β-scission [14]. A relatively sharp transition between oligomerization and alkylation activity has been observed with sulfuric acid at H_0 values between -8.0 and -8.5 [45].

Using triflic acid modified with trifluoroacetic acid or water, Olah et al. [46] found the best alkylation conditions at an acid strength of about $H_0 = -10.7$. Pure triflic acid with $H_0 = -14.1$ led mainly to cracked products, while diluted triflic acid ($H_0 > -10.7$) favored oligomerization [46]. Similarly, the dilution of various liquid acids with carbon dioxide has been explored. While very strong acids such as triflic acid produce higher quality alkylate upon dilution with the weak base CO_2, slightly weaker acids such as sulfuric acid performed better without CO_2 [47]. The different H_0 values for the transition from alkylation to oligomerization with sulfuric and triflic acid suggest that the acid strength is not the only factor determining the reactivity of the carbenium ions.

Similar results are obtained for solid acids. The high cracking activity of very strong solid acids was shown by Corma et al. [48], who compared sulfated zirconia and zeolite BEA at reaction temperatures of 0 and 50 °C in isobutane/2-butene alkylation. While BEA catalyzed mainly dimerization at 0 °C, sulfated zirconia exhibited a high selectivity to trimethylpentanes. At 50 °C, on the other hand, zeolite BEA produced more TMPs than sulfated zirconia, which under these conditions produced mainly cracked products (65 wt% selectivity). The TMP/DMH ratio was, however, always higher for the sulfated zirconia sample. These distinctive differences in the product distribution are attributed to the much stronger acid sites in sulfated zirconia as compared to zeolite BEA. The strong acid sites in sulfated zirconia preferentially catalyzed alkane cracking, and allowed hydride transfer at lower temperatures than the zeolitic acid sites [48].

Resembling the behavior of dilute liquid acids, zeolites with weak Brønsted acid sites catalyze mainly oligomerization reactions. This is shown by a comparison of the isostructural zeolites H-SAPO-37 and H-FAU as alkylation catalysts. The H-FAU investigated had a much higher relative concentration of strong acid sites than H-SAPO-37. Therefore, H-SAPO-37 mainly catalyzed dimerization, with a small amount of 3,4-DMH as the most abundant saturated compound. H-FAU produced mainly TMPs [49].

Fundamentally different from liquid acids, zeolites encompass different populations of sites varying substantially in nature and strength. In contrast, liquid acids with a certain composition have a well-defined acid strength. Depending on the type of zeolite, its aluminum content, and the exchange procedure, Brønsted and Lewis acid sites with a wide range of strength and concentration are present. Therefore, we have carried out a number of studies to separate the impact of each parameter on the alkylation performance.

When leaving all other parameters constant, the lifetime of zeolitic alkylation catalysts depends on the concentration of Brønsted acid sites. This was shown by using a series of zeolite H-BEA with varying ratios of Brønsted acid sites to Na^+ cations. The decrease in the concentration of Brønsted acid sites led to a parallel decrease in the catalyst lifetime for alkylation [33].

In a recent study, a series of rare-earth exchanged faujasites were tested as alkylation catalysts in a continuously operated stirred tank reactor [10]. The analysis of the time-on-stream behavior of these catalysts showed that hydride transfer and cracking activity stopped abruptly, when the olefin concentration exceeded 0.1 wt%. This is shown in Figs. 3a and 3b. Most saturated compounds (with the exception of 3,4-DMH) ceased being produced when the conversion started to drop. This suggests a parallel progress of the deactivation with respect to all active sites in the reactor as long as they are exposed to identical reaction conditions (a feature, which is unique for CSTR-type reactors). On the individual site, this means that the rates of hydride transfer and cracking drop within a very short time interval. Oligomerization (including dimerization) is then the only proceeding reaction. This confirms the existence of two different active sites in zeolites during alkylation, i.e., strong sites catalyzing alkylation and cracking, which involve hydride transfer and weak acid sites catalyzing oligomerization, which allow the oligomers to desorb without hydride transfer. The heavy alkylate C_{9+} products originate from multiple alkylation on the stronger sites and the incorporated oligomerization products formed at weaker sites as long as hydride transfer and olefin addition on those stronger acid sites are catalyzed. When the strong sites are deactivated, multiple alkylation and the incorporation of the larger olefins ceases, while oligomerization still proceeds on the weaker sites. This is reflected in the changing slope of the C_{9+} curve in Fig. 3a (due to unsaturated compounds) and the formation of octenes seen in Fig. 3b.

Catalysts with high concentrations of weak acid sites, therefore, have a tendency to produce large amounts of octenes and higher oligomers. As long as the Brønsted acid sites catalyzing hydride transfer are active, the olefins formed in this way are included in the alkylation cycle. However, this accelerates the formation of heavy alkylate, which eventually blocks the active sites. Consequently, the lower the concentration of weak acid sites, the longer the catalyst will be active. This is reflected in the correlation between the lifetimes with respect to alkylation and the ratio of the number of strong Brønsted acid sites to the total number of Brønsted acid sites (the total concentration of Brønsted acid sites is measured by pyridine sorption at 100 °C; the concentration of strong Brønsted acid sites is measured by pyridine sorption at 450 °C). This correlation is displayed in Fig. 4a. Additionally, a correlation was found

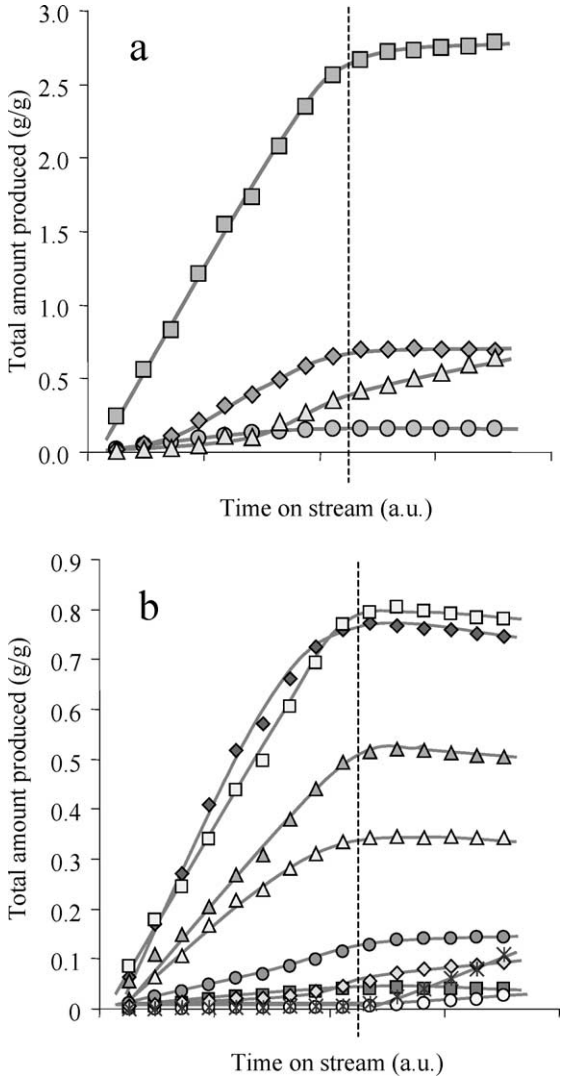

Fig. 3. Alkylation performance of catalyst RE-FAU. (a) Total amount of the different product groups with time on stream (○ *n*-butane, ◇ C_5–C_7 products, □ C_8 products, △ C_{9+} products); (b) total amounts of the individual C_8 products with time on stream (◆ 2,2,4-TMP, ■ 2,5-DMH/2,2,3-TMP, ▲ 2,4-DMH, ▲ 2,3,4-TMP, □ 2,3,3-TMP, ● 2,3-DMH, ○ 4-MHp/3,4-DMH, ◇ 3,4-DMH, ✳ octenes). The dashed line represents the end of the lifetime of the catalyst.

between the ratio of the concentrations of strong Brønsted acid sites and Lewis acid sites (B/L ratio) and the catalyst lifetimes. With increasing ratios of Brønsted to Lewis acid sites, the catalyst lifetimes increased.

Similarly, Lewis acid sites are negative for the alkylation performance. The correlation is directly proportional to the fraction of Brønsted acid sites among all acid sites (B/(B + L) ratio), which is shown in Fig. 4b. They influence the alkylation reaction by adsorbing alkenes and, in this way increase the alkene concentration near Brønsted acid sites. This increases the probability of further alkene addition leading to accelerated deactivation.

It has also been claimed that the presence of strong Lewis acid sites promotes the formation of unsaturated com-

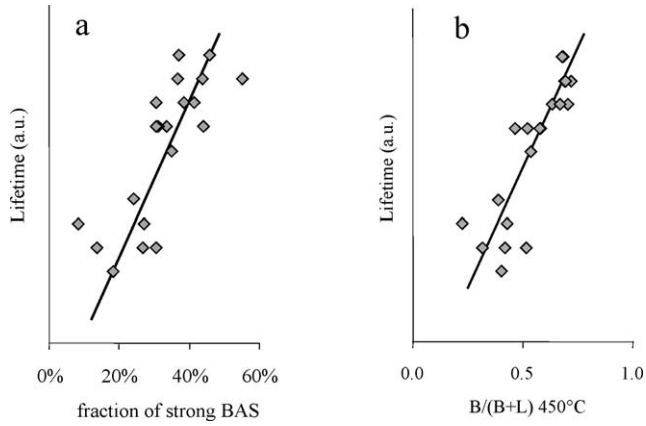

Fig. 4. Acidity–lifetime correlations found with zeolite RE-FAU. (a) Catalytic lifetime as a function of the fraction of strong Brønsted centers; (b) catalytic lifetime of the individual samples as a function of the Brønsted/(Brønsted + Lewis) ratio measured at 450 °C.

pounds [50]. Flego et al. [51], studying the deactivation of a La-H-FAU zeolite in isobutane/1-butene alkylation, demonstrated the preferred formation of unsaturated carbenium ions with increased Lewis acidity. Increasing catalyst activation temperatures leads to higher Lewis acid site concentrations, which increase the formation of mono- and dienylic carbenium ions. Thus, it is important to have a high concentration of strong Brønsted and a low concentration of Lewis acid sites.

When relating the integral yields to the different product groups (integrated over the time of complete butene conversion) against the catalyst lifetimes, differences between alkylation catalysts are obvious. With increasing catalyst lifetime the yield of heavy alkylate decreases, while octane and *n*-butane yields increase (see Fig. 5a). The increasing *n*-butane yield is attributed to higher rates of hydride transfer between *n*-butyl carbenium ions and isobutane. The formed isobutyl carbenium ions partly decompose to isobutene and free acid sites. On average, such a cycle occurs 4 to 5 times per acid site during the usable lifetime of the catalysts. This model is further supported by the parallel increase of the 2,2,4-trimethylpentane yields, which result from the alkylation of the isobutyl carbenium ions by isobutene (see Fig. 5b).

It should be emphasized here that high 2,2,4-TMP selectivities are not necessarily a sign of high hydride transfer activity. Zeolite BEA produces 2,2,4-TMP sometimes with over 50 wt% selectivity [52–54]. In contrast to the high-alumina faujasites, the selectivity to *n*-butane is low with zeolite BEA. In this case, the high selectivity to 2,2,4-TMP is related to low rates of hydride transfer relative to the methyl shift isomerization of the trimethylpentanes. This favors high selectivity to the most stable isomer, i.e., 2,2,4-trimethylpentane. The slower hydride transfer rate suggests that the formation of the new carbon–oxygen bond is more important than the polarity of the C–O bond in the existing alkoxy group. Additionally, the differences in the pore structure could also induce variations in the rate of

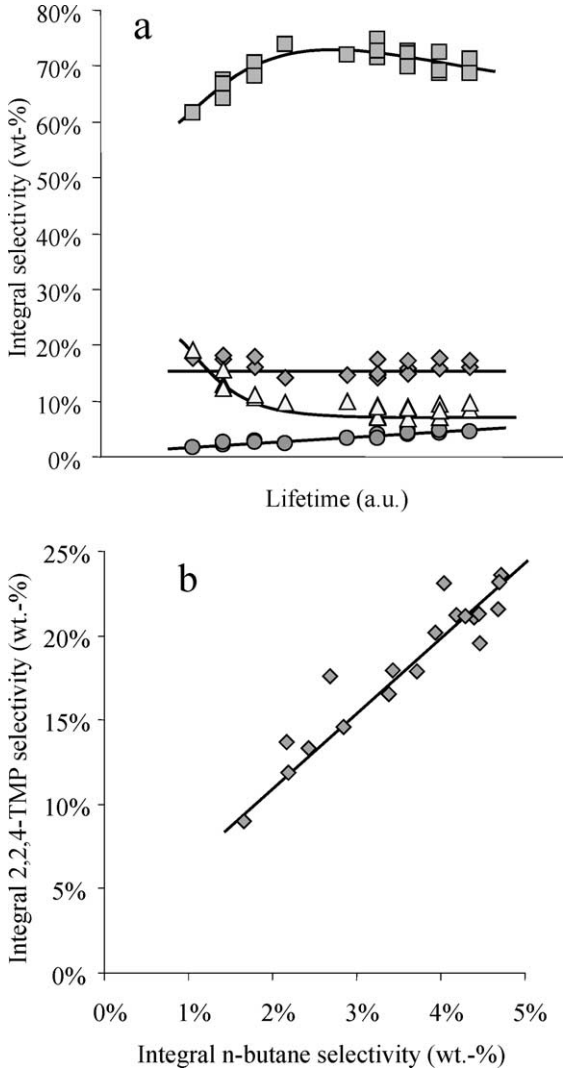

Fig. 5. Changes in selectivities with the lifetimes of the individual RE-FAU samples. (a) Integral selectivities to the different product groups as a function of the lifetimes of the individual samples (○ *n*-butane, ◇ C_5–C_7 products, □ C_8 products, △ C_{9+} products); (b) integral selectivity to 2,2,4-TMP as a function of the integral selectivity to *n*-butane. In both graphs, each data point represents a single alkylation experiment.

the hydride transfer. Note that high rates of hydride transfer in zeolites with low Si/Al ratios have also been observed for alkane cracking [27,55,56].

5. Deactivation pathways

All liquid acids produce conjunct polymers as alkylation byproducts, although the amounts produced differ substantially. These polymers are also named acid-soluble oil (ASO) or red oil, because they are found in the acid phase and exhibit a dark red color. They dilute the acid and, thus, lower the acid strength, so that in a continuous process a slipstream of used acid has to be withdrawn and replenished by fresh acid.

The oil is a complex mixture of highly branched hydrocarbons with single and conjugated double bonds and rings containing five and six carbon atoms. The individual compounds have molecular weights in the range of 265–360 [57]. With triflic acid [58] or sulfuric acid [44] the polymers are strongly bound to the acid in the form of the corresponding esters. Hydrofluoric acid should behave accordingly. With all liquid acids, the composition of the polymers is largely independent of the feed.

Zeolites and other solid acids deactivate by the buildup of a polymer, which eventually blocks the pores of the catalyst. Deactivation can be slowed down by choosing appropriate reaction conditions and by reactor design, but eventually all catalysts have to be regenerated. To characterize the deposits and the deactivated catalysts, a wide variety of methods have been employed, ranging from ^{13}C NMR [51,59,60] and ^{1}H NMR [61] to mass spectrometry (also in combination with gas chromatography) [61–63], IR-spectroscopy [50,51,53,61], and UV–vis [51,64].

The parallel characterization of deactivated alkylation catalysts by solid-state ^{13}C NMR, IR, and UV–vis reveals the low sensitivity of ^{13}C NMR and IR to detect unsaturated compounds, which are readily observed by UV–vis spectroscopy [51]. This low sensitivity has led to the frequent conclusion that the deposits consist mainly of long-chain branched alkanes. Such conclusions were drawn although the H/C ratio was as low as 1.8, which in a C_{20} molecule already represents three carbon–carbon double bonds. Mass spectrometric analysis of extracted coke [61,62] led to similar results concerning the degree of unsaturation and the general structure of the molecules. C_{15}–C_{20} compounds with 2–4 unsaturations/cycles were found to dominate. After hydrogenation, the general formula suggested a naphtenic structure with one or two five- and six-rings. Note that these compounds closely resemble the conjunct polymers in liquid acid-catalyzed alkylation having also the same range of molecular weights.

In order to explore the role of the reaction temperature (40–130 °C) on the carbon deposits formed, deactivated rare-earth exchanged FAU based alkylation catalysts were examined [9]. Using UV–vis, GC-MS, and ^{1}H NMR spectroscopy to characterize the deposits (obtained by a complete digestion of the zeolite in aqueous HF and a subsequent extraction with hexane), the highly unsaturated nature of the deposits was verified. Even with low reaction temperatures, the catalysts produced a small amount of aromatics. The concentration of aromatic molecules in the deposit steeply increased with the reaction temperature, while the degree of branching (CH_3/CH_2 ratio) markedly decreased. The quantitative analysis of the ^{1}H NMR of the deposits formed at different reaction temperatures is shown in Fig. 6. The GC-MS measurements also showed that a considerable part of the low-temperature deposit consists of alkanes and alkenes, i.e., of simple alkylation products (the alkoxides on the acid sites lead to alkenes when the zeolite is dissolved). The adsorbed species, thus, only partly resemble the conjunct polymers formed in liquid-acid-catalyzed alkylation.

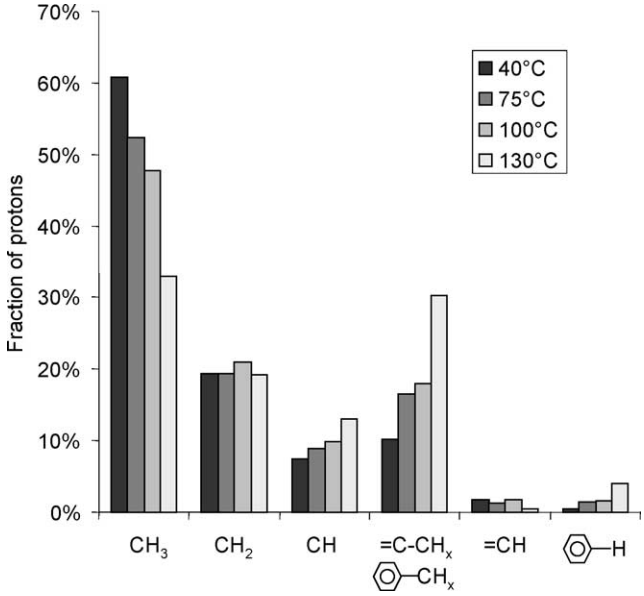

Fig. 6. Fraction of protons in the different functional groups as measured with ^{1}H NMR on the deposits from reactions of RE-FAU at 40, 75, 100, and 130 °C.

Formation of the unsaturated molecules under the relatively mild conditions of alkylation seems puzzling at first. However, alkenes formed by dimerization or cracking appear to undergo multiple hydride transfer steps using hydrogen at tertiary carbon atoms. Finally, cyclization of the multiply unsaturated molecule occurs [see reaction steps (3) and (4)]. Note that each step also produces a saturated molecule (represented here as isobutane) next to the carbenium ion:

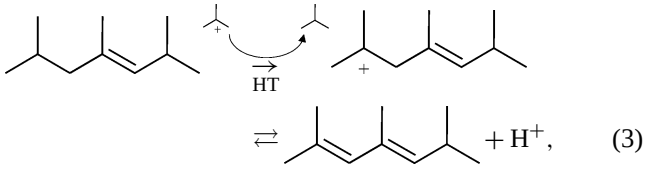

(3)

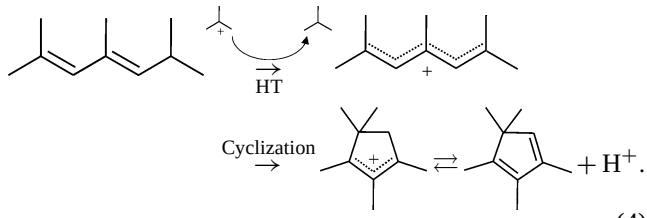

(4)

These cycloalkenyl carbenium ions, especially the cyclopentenyl cations, are very stable [65,66] and have been observed as free cations in zeolites [67,68]. Obviously, the reaction does not stop with the cycloalkenyl ions, as benzene rings are also found in the deposits. Presumably, a relatively high energy barrier has to be overcome to form the benzenium ion, as the steep increase in aromatic protons with reaction temperature (see Fig. 6) suggests.

The chemical reactivity of these deposits depends subtly upon the reaction conditions. Nitrogen adsorption on deactivated catalysts at 77 K (a temperature at which the adsorbed molecules are very rigid) shows that the micropore system of a deactivated catalyst is completely filled/blocked. At 373 K, however, pyridine enters the pore system and replaces a significant fraction of the adsorbed hydrocarbons forming pyridinium ions on nearly 70% of the Brønsted acid sites. This is shown in Fig. 7, in which the pyridine adsorption capacity of fresh and deactivated zeolites RE-FAU and H-BEA is compared. The replacement of adsorbed hydrocarbons by pyridine in the deactivated samples is demonstrated by the negative bands in the C–H bending region. A similar observation was made with zeolites deactivated in the *m*-xylene transformation [69].

The theoretical description for this was given by Song et al. [70], who studied the 1,3-dimethylcyclopentenyl carbenium ion ($C_7H_{11}^+$) adsorbed on H-ZSM-5. Coadsorption of basic molecules led to a deprotonation of the carbenium ion to form the neutral diene, when the employed base had

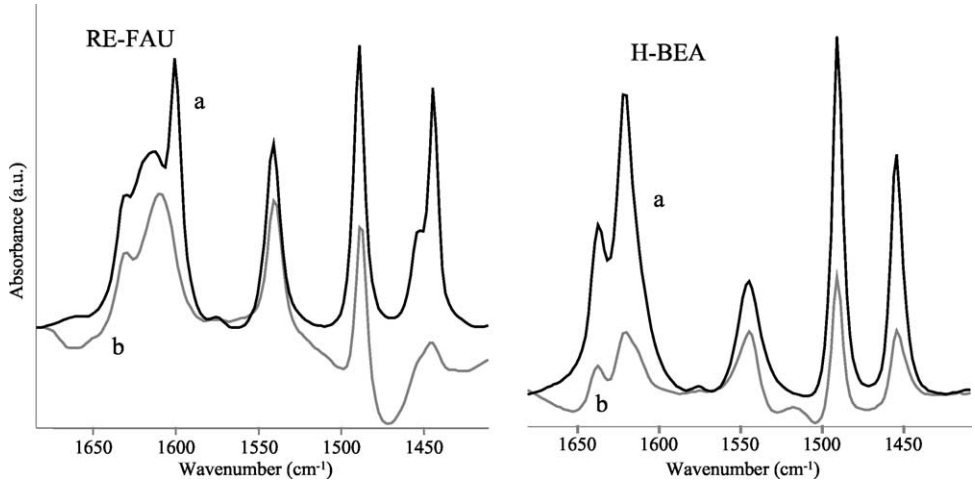

Fig. 7. Difference spectra of adsorbed pyridine on RE-FAU and H-BEA in (a) fresh and (b) deactivated state at 100 °C. Note that hydrocarbon bands at 1650, 1530, 1505, and 1470 cm^{-1} were reduced in intensity after pyridine adsorption on the deactivated samples.

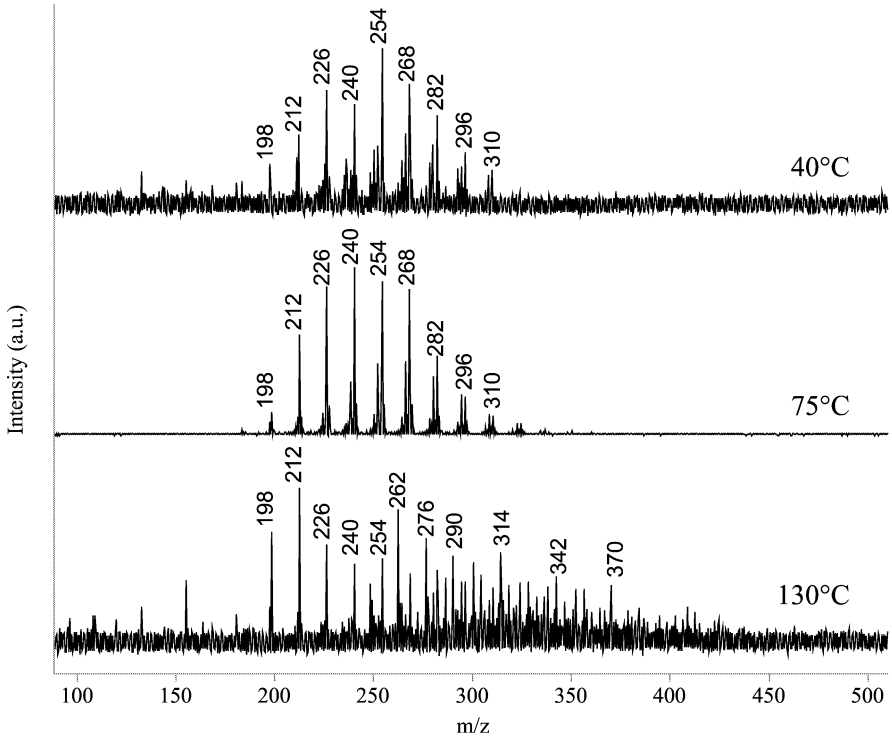

Fig. 8. LDI-TOF mass spectra of deactivated RE-FAU samples used in reactions at 40, 75, and 130 °C.

a proton affinity higher than the deprotonation enthalpy of the dimethylcyclopentenyl ion [70]; i.e., only those reactions will be thermodynamically favored that produce more stable carbenium ions.

Hydride transfer from isobutane (the most abundant hydride transfer agent) to a substituted cyclopentenyl ion to yield an isobutyl carbenium ion should therefore be unfavorable. Thus, once a Brønsted acid site is occupied by a cycloalkenyl ion, it is blocked for the catalytic alkylation cycle, which seems to be the dominating mechanism at high reaction temperatures. At low reaction temperatures, the catalysts produce less unsaturated compounds and, hence, appear to deactivate by pore blocking through formation of bulky heavy alkylate.

While the studies discussed allowed to characterize the relative abundance of functional groups in the deactivated molecular sieves, the molecular mass of the unsaturated molecules is not accurately detected in that way. For this purpose laser desorption ionization time of flight mass spectrometry (LDI-TOF MS) was applied. The technique is excellently suited to vaporize and analyze large molecules without fragmentation (see, e.g., [71]).

The LDI-TOF mass spectra of the deactivated catalysts used in reactions at 40, 75, and 130 °C are shown in Fig. 8. The spectra of the samples used at 40 and 75 °C are very similar and exhibit a molecular weight distribution between 180 and 340 Da. The main peaks are 14 Da apart, which is characteristic of a CH_2 group. The detected compounds are based on a C_nH_{2n-12} formula, which could be explained by a naphthalene molecule with an increasing number and/or length of side chains. The deactivated sample from the reaction at 130 °C had a broader distribution (between 180 and 430 Da) and showed additional masses with higher hydrogen deficiencies, in line with the higher aromaticity detected by NMR, UV–vis, and GC-MS. The mass distribution detected by LDI-TOF MS with all samples is in close agreement with the distribution measured by GC-MS. However, the presence of both aliphatic and aromatic molecules in the deposits complicated the assignment of individual masses to certain types of compounds.

6. The effect of process parameters upon catalyst performance

As with all catalytic reactions, a close interconnection exists between the catalytic performances, the catalyst properties, and the operation conditions. Important parameters that have been also partly discussed include the reaction temperature, feed paraffin/olefin ratio, olefin space velocity, olefin feed composition, and reactor type. Note that while the variations of these parameters induce similar effects independent of the chosen catalyst, the sensitivity on a particular parameter strongly depends upon the catalyst.

Table 1 summarizes the most important parameters employed in industrial operations for different acids. The numbers for the liquid acids are taken from references [72–74], while the values given for zeolites are averages of several patents and own experience. Two points have to be emphasized here: (i) Zeolites can be successfully operated at the same severity (with respect to P/O and OSV) as the liquid acids, or higher. (ii) The catalyst productivity of zeolites

Table 1
Typical values of important process parameters

	HF	H_2SO_4	Zeolites
Reaction temperature (°C)	16–40	4–16	50–100
Feed paraffin/olefin ratio (mol/mol)	11–14	7–10	6–15
Olefin space velocity (kg_{Olefin}/kg_{Acid} h)	0.1–0.6	0.03–0.2	0.2–1.0
Exit acid strength (wt%)	83–92	89–93	–
Acid per reaction volume (vol%)	25–80	40–60	20–30
Catalyst productivity ($kg_{Alkylate}/kg_{Acid}$)	1000–2500	6–18	4–20

The numbers for the liquid acids are taken from Refs. [72–74]. As zeolites are not used industrially so far, the given values represent the authors' views on realistic numbers for future industrial operation in a slurry reactor.

is on the same order of magnitude as that of sulfuric acid. Comparing the intrinsic activity of zeolites (0.5–3 mmol acid sites per gram acid) with that of sulfuric acid (20 mmol acid sites per gram acid), Brønsted acid sites in zeolites actually outperform protons in sulfuric acid. Nevertheless, as zeolite-based catalysts are expected to be significantly more expensive than sulfuric acid, the potential impact of operating and regeneration conditions will be discussed in detail.

Zeolites have to be operated at reaction temperatures significantly higher than those for the liquid acids. This is due to the lower acid strength of zeolites and/or solvation effects in sulfuric and hydrofluoric acid resulting in higher activation energies for the individual reaction steps in zeolites. Efficient micropore diffusion also requires higher temperatures. The temperature optimum is therefore between 50 to 100 °C. Catalysts produce increasing fractions of cracked products with increasing reaction temperature [10,52,53,75], and the TMP/DMH ratio decreases with increasing temperature. However, a decrease in heavy-end selectivity with increasing temperature [53] and an increase [10,52] have been reported. Intuitively, one would assume that due to the order of activation energies (cracking > hydride transfer > oligomerization; see Ref. [39]), oligomerization would dominate at low temperatures. Heavy compounds may well be produced at low temperatures, but due to low diffusivity only a small part leaves the pores and appears in the product.

These diffusion problems have stimulated research on the application of supercritical conditions to overcome a buildup of heavy molecules in the catalyst pores. It has been argued that under such conditions, the bulky molecules deactivating the catalyst should be more efficiently removed from the catalyst pores.

The feed itself can be employed as a supercritical medium, but the critical point of isobutane is at 135 °C and 36.5 bar. As discussed above, alkylation under these conditions leads to excessive cracking and to highly unsaturated and aromatic deposits. Indeed, aromatic molecules were also detected by He and He exploring supported heteropolyacids at 137 °C as alkylation catalysts [76]. The catalysts stay active for longer TOS as compared to conventional operation, but a substantial amount of olefinic products [77,78] has been observed.

Carbon dioxide has been used as a diluent to reduce the high reaction temperatures needed with supercritical isobutane. The results of Clark and Subramaniam [79] and Santana and Akgerman [80] show that a stable conversion can indeed be maintained with a 10-fold excess of carbon dioxide at 50 °C and 155 bar. However, the conversion was very low (< 20 wt%) and the product contained only minor amounts of trimethylpentanes, i.e., dimerization dominated over alkylation. Ginosar et al., testing a variety of supercritical solvents on a variety of different solid acids came to the conclusion that working under supercritical conditions generally does not improve the alkylation performance [81].

The crucial parameter that ensures high alkylate quality and a low acid consumption is the ratio between the rates of hydride transfer and oligomerization. This ratio should be as high as possible. With high isobutane concentrations the carbenium ion has a higher probability to react with an isobutane molecule to form the desired product via hydride transfer rather than to react with another alkene. Two process parameters influence the ratio between hydride transfer and repeated olefin addition, i.e., the feed paraffin/olefin (P/O) ratio and the olefin space velocity (OSV). The P/O ratio determines the concentration of isobutane in the reactor, which in turn determines the rate of hydride transfer.

A detailed study of the influence of the P/O ratio and OSV on the performance of zeolite H-BEA in a CSTR has been published by de Jong et al. The authors developed a simple kinetic model, which was able to predict catalyst lifetimes as a function of P/O and OSV. Catalyst lifetimes increased with increasing P/O and decreasing OSV. Additionally, the authors impressively proved the superiority of CSTR over PFR technology [31]. Taylor and Sherwood [75], employing a USY zeolite in a CSTR, obtained qualitatively similar results. The authors stress the detrimental effect of unreacted alkene on lifetime and product quality [75]. Note that in our own studies using rare-earth-exchanged FAU-based catalysts and a CSTR, the catalyst productivity was nearly independent of the OSV. At higher OSV the catalyst lifetime was shorter, but in this shorter time the same total amount of alkylate was produced. The P/O had only a moderate influence on the catalytic performance, which is attributed to mixing problems [10].

7. Conclusions

The catalytic chemistry of the alkylation reaction with liquid and solid acid catalysts is governed by the same principles. Differences in the importance of individual steps originate from the variety of possible structures and acidity distributions of solid acids. Hydride transfer is the crucial step that determines the product distribution and the productivity of the catalyst. Hydride transfer is favored in catalysts with a high concentration of strong Brønsted acid sites and a low concentration of Lewis acid sites. For maintaining high product quality and long lifetimes, it is crucial to operate at very high internal paraffin/olefin ratios, which can be achieved by employing back-mixed reactors. All cat-

alysts eventually deactivate by a buildup of highly unsaturated polymers, which are strongly bound to the acid sites, with both liquid and solid acids. With solid acids, however, the regeneration seems capable of overcoming the apparent high price barriers currently preventing commercial application of solid acid catalysts.

Acknowledgments

The authors thank Professor V. Kazansky, Dr. S.M. Csicsery, and Dr. H.J. Räder for helpful discussions. Partial financial support from Süd-Chemie AG is gratefully acknowledged.

References

[1] J. Stell, Oil Gas J. 99 (52) (2001) 74.
[2] L.F. Albright, Chemtech July (1998) 46.
[3] F.W. Kirsch, J.D. Potts, D.S. Barmby, J. Catal. 27 (1972) 142.
[4] W.E. Garwood, P.B. Venuto, J. Catal. 11 (1968) 175.
[5] T. Chang, Oil Gas J. 98 (35) (2000) 17.
[6] S.I. Hommeltoft, Appl. Catal. A 221 (2001) 421.
[7] A. Corma, A. Martinez, Catal. Rev.-Sci. Eng. 35 (1993) 483.
[8] J. Weitkamp, Y. Traa, in: G. Ertl, H. Knözinger, J. Weitkamp (Eds.), Handbook of Heterogeneous Catalysis, Vol. 4, VCH, Weinheim, 1997, p. 2039.
[9] A. Feller, J.O. Barth, A. Guzman, I. Zuazo, J.A. Lercher (2002), submitted for publication.
[10] A. Feller, A. Guzman, I. Zuazo, J.A. Lercher (2002), submitted for publication.
[11] S.I. Hommeltoft, O. Ekelund, J. Zavilla, Ind. Eng. Chem. Res. 36 (1997) 3491.
[12] M.V. Frash, V.N. Solkan, V.B. Kazansky, J. Chem. Soc. Faraday Trans. 93 (1997) 515.
[13] V.B. Kazansky, H.C.L. Abbenhuis, R.A. van Santen, M.L.V. Vorstenbosch, Catal. Lett. 69 (2000) 51.
[14] V.B. Kazansky, Catal. Rev.-Sci. Eng. 43 (2001) 199.
[15] L.F. Albright, M.A. Spalding, J.A. Nowinski, R.M. Ybarra, R.E. Eckert, Ind. Eng. Chem. Res. 27 (1988) 381.
[16] V.B. Kazansky, Catal. Today 51 (1999) 419.
[17] R.J. Gorte, D. White, Topics Catal. 4 (1997) 57.
[18] V.B. Kazansky, in: G. Ertl, H. Knözinger, J. Weitkamp (Eds.), Handbook of Heterogeneous Catalysis, Vol. 2, VCH, Weinheim, 1997, p. 740.
[19] A.M. Rigby, G.J. Kramer, R.A. van Santen, J. Catal. 170 (1997) 1.
[20] H. Hogeveen, C.J. Gaasbeek, A.F. Bickel, Rec. Trav. Chim. 88 (1969) 703.
[21] G.A. Olah, J.A. Olah, in: G.A. Olah, P.R. Schleyer (Eds.), Carbonium Ions, Vol. 2, Interscience, New York, 1970, p. 715.
[22] C.J.A. Mota, P.M. Esteves, A. Ramirez-Solis, R. Hernandez-Lamoneda, J. Am. Chem. Soc. 119 (1997) 5193.
[23] M.A. Sanchez-Castillo, N. Agarwal, C. Miller, R.D. Cortright, R.J. Madon, J.A. Dumesic, J. Catal. 205 (2002) 67.
[24] G.A. Olah, Angew. Chem. 85 (1973) 183.
[25] G.A. Olah, Y.K. Mo, J.A. Olah, J. Amer. Chem. Soc. 95 (1973) 4939.
[26] G.A. Olah, G.K.S. Prakash, in: S. Patai, Z. Rappoport (Eds.), The Chemistry of Alkanes and Cycloalkanes, Wiley, London, 1992, p. 609.
[27] K.A. Cumming, B.W. Wojciechowski, Catal. Rev.-Sci. Eng. 38 (1996) 101.
[28] L. Schmerling, J. Am. Chem. Soc. 67 (1945) 1778.
[29] L. Schmerling, J. Am. Chem. Soc. 68 (1946) 275.
[30] L. Lee, P. Harriott, Ind. Eng. Chem. Process Des. Dev. 16 (1977) 282.
[31] K.P. de Jong, C.M.A.M. Mesters, D.G.R. Peferoen, P.T.M. van Brugge, C. de Groot, Chem. Eng. Sci. 51 (1996) 2053.
[32] M.F. Simpson, J. Wei, S. Sundaresan, Ind. Eng. Chem. Res. 35 (1996) 3861.
[33] G.S. Nivarthy, K. Seshan, J.A. Lercher, Micropor. Mesopor. Mater. 22 (1998) 379.
[34] P. Ausloos, S.G. Lias, J. Am. Chem. Soc. 92 (1970) 5037.
[35] M. Meot-Ner, F.H. Field, J. Chem. Phys. 64 (1976) 277.
[36] M. Meot-Ner, J. Am. Chem. Soc. 109 (1987) 7947.
[37] J.A. Sunner, K. Hirao, P. Kebarle, J. Phys. Chem. 93 (1989) 4010.
[38] M. Boronat, P. Viruela, A. Corma, J. Phys. Chem. A 102 (1998) 9863.
[39] G. Yaluris, J.E. Rekoske, L.M. Aparicio, R.J. Madon, J.A. Dumesic, J. Catal. 153 (1995) 54.
[40] H.C. Beirnaert, J.R. Alleman, G.B. Marin, Ind. Eng. Chem. Res. 40 (2001) 1337.
[41] F. Eder, J.A. Lercher, Zeolites 18 (1997) 75.
[42] J. Jänchen, H. Stach, L. Uytterhoeven, W.J. Mortier, J. Phys. Chem. 100 (1996) 12489.
[43] F. Eder, J.A. Lercher, J. Phys. Chem. 100 (1996) 16460.
[44] L.F. Albright, M.A. Spalding, C.G. Kopser, R.E. Eckert, Ind. Eng. Chem. Res. 27 (1988) 386.
[45] M.Y. He, E. Min, Catal. Today 63 (2000) 113.
[46] G.A. Olah, P. Batamack, D. Deffieux, B. Török, Q. Wang, A. Molnar, G.K. Surya Prakash, Appl. Catal. A 146 (1996) 107.
[47] G.A. Olah, E. Marinez, B. Török, G.K.S. Prakash, Catal. Lett. 61 (1999) 105.
[48] A. Corma, M.I. Juan-Rajadell, J.M. Lopez-Nieto, A. Martinez, C. Martinez, Appl. Catal. A 111 (1994) 175.
[49] H.B. Mostad, M. Stöcker, A. Karlsson, T. Rørvik, Appl. Catal. A 144 (1996) 305.
[50] F.A. Diaz-Mendoza, L. Pernett-Bolano, N. Cardona-Martinez, Thermochim. Acta 312 (1998) 47.
[51] C. Flego, I. Kiricsi, W.O. Parker Jr., M.G. Clerici, Appl. Catal. A 124 (1995) 107.
[52] A. Corma, V. Gomez, A. Martinez, Appl. Catal. A 119 (1994) 83.
[53] G.S. Nivarthy, Y. He, K. Seshan, J.A. Lercher, J. Catal. 176 (1998) 192.
[54] G.S. Nivarthy, A. Feller, K. Seshan, J.A. Lercher, Stud. Surf. Sci. Catal. 130 (2000) 2561.
[55] A. Corma, A.V. Orchillés, Micropor. Mesopor. Mater. 35–36 (2000) 21.
[56] A.F.H. Wielers, M. Vaarkamp, M.F.M. Post, J. Catal. 127 (1991) 51.
[57] L. Miron, R.J. Lee, J. Chem. Eng. Data 8 (1963) 150.
[58] A.S. Berenblyum, L.V. Ovsyannikova, E.A. Katsman, J. Zavilla, S.I. Hommeltoft, Y.Z. Karasev, Appl. Catal. A 232 (2002) 51.
[59] J. Weitkamp, S. Maixner, Zeolites 7 (1987) 6.
[60] M. Stöcker, H. Mostad, T. Rørvik, Catal. Lett. 28 (1994) 203.
[61] J. Pater, F. Cardona, C. Canaff, N.S. Gnep, G. Szabo, M. Guisnet, Ind. Eng. Chem. Res. 38 (1999) 3822.
[62] R. Schöllner, H. Hölzel, Z. Chem. 15 (1975) 469.
[63] K. Yoo, E.C. Burckle, P.G. Smirniotis, Catal. Lett. 74 (2001) 85.
[64] I. Kiricsi, C. Flego, G. Bellussi, Appl. Catal. A 126 (1995) 401.
[65] N.C. Deno, in: G.A. Olah, P.R. Schleyer (Eds.), Carbonium Ions, Vol. 2, Interscience, New York, 1970, p. 783.
[66] T.S. Sorensen, in: G.A. Olah, P.R. Schleyer (Eds.), Carbonium Ions, Vol. 2, Interscience, New York, 1970, p. 807.
[67] J.B. Nicholas, J.F. Haw, J. Am. Chem. Soc. 120 (1998) 11,804.
[68] S. Yang, J.N. Kondo, K. Domen, Catal. Today 73 (2002) 113.
[69] H.S. Cerqueira, P. Ayrault, J. Datka, M. Guisnet, Micropor. Mesopor. Mater. 38 (2000) 197.
[70] W. Song, J.B. Nicholas, J.F. Haw, J. Am. Chem. Soc. 123 (2001) 121.
[71] J.K. Pruns, J.P. Vietzke, M. Strassner, C. Rapp, U. Hintze, W.A. König, Rapid Commun. Mass Spectrom. 16 (2002) 208.
[72] J.H. Gary, G.E. Handwerk, in: L.F. Albright, R.N. Maddox, J.J. McKetta (Eds.), Petroleum Refining—Technology and Economics, Dekker, New York, 1979, p. 142.
[73] S. Kinnear, in: Proceedings of the STRATCO Alkylation Seminar, Phoenix, Arizona, 1998.

[74] S. Ackerman, G.K. Chitnis, D.S. McCaffrey Jr., Prepr. Div. Pet. Chem. Am. Chem. Soc. 46 (2001) 241.
[75] R. Taylor, D.E. Sherwood Jr., Appl. Catal. A 155 (1997) 195.
[76] Y. He, Y. He, Catal. Today 74 (2002) 45.
[77] L. Fan, I. Nakamura, S. Ishida, K. Fujimoto, Ind. Eng. Chem. Res. 36 (1997) 1458.
[78] I. Nakamura, S. Ishida, K. Fujimoto, Prepr. Div. Pet. Chem. Am. Chem. Soc. 40 (1995) 512.
[79] M.C. Clark, B. Subramaniam, Ind. Eng. Chem. Res. 37 (1998) 4.
[80] G.M. Santana, A. Akgerman, Ind. Eng. Chem. Res. 40 (2001) 3879.
[81] D.M. Ginosar, D.N. Thompson, K. Coates, D.J. Zalewski, Ind. Eng. Chem. Res. 41 (2002) 2864.